



Direct observation of the F region dynamo currents and the spatial structure of the EEJ by CHAMP

Hermann Lühr¹ and Stefan Maus²

Received 5 October 2006; revised 8 November 2006; accepted 17 November 2006; published 20 December 2006.

[1] The satellite CHAMP in its low-altitude polar orbit, and with its high-resolution magnetic field measurements, provides the opportunity to investigate ionospheric currents in great detail. In this study we focus on average features of equatorial current systems during day time. Considering quiet time observations from the period Aug. 2000 to Oct. 2004 we determined the mean spatial structure of the EEJ current. The existence of reverse currents at the flanks of the primary eastward current is confirmed. More importantly, average characteristics of the F region dynamo driven currents are observed for the first time throughout the daytime. The meridional current system, driven by westward thermospheric winds, peaks around noon. Similar meridional currents, but flowing in the opposite sense, are observed at the dusk sector. At CHAMP altitudes we find over the dip equator in the F region a vertical sheet current of about 6 mA/m oriented downward at noon and an upward current of 4 mA/m around sunset. **Citation:** Lühr, H., and S. Maus (2006), Direct observation of the F region dynamo currents and the spatial structure of the EEJ by CHAMP, *Geophys. Res. Lett.*, 33, L24102, doi:10.1029/2006GL028374.

1. Introduction

[2] Electrodynamical processes in the equatorial ionosphere are characterized by the special geometry of the geomagnetic field in this region. Quite different effects are observed at E and F region altitudes. The equatorial electrojet (EEJ) is a ribbon of intense electric currents in the ionospheric E region following the dip equator. Although the horizontal eastward current is the most prominent part there are other EEJ associated currents such as the reverse and the meridional currents. Reverse currents flowing at the flanks of the EEJ were deduced from ground observations [e.g., *Fambitakoye and Mayaud*, 1976] and also identified in satellite measurements [Lühr *et al.*, 2004]. The existence of meridional currents was predicted by Untiedt [1967]. His model was later improved by Sugiura and Poros [1969]. They predicted upward currents above the dip equator and a divergence of these currents into both hemispheres along magnetic field lines. Currents return to the equator at the E region base. Such current loops caused by the height-dependence of the Hall/Pedersen conductivity ratio are expected to be strongest at altitudes of 120 to 130 km in the noon time sector. These meridional currents

cannot be observed from ground. Their determination requires measurements inside the loop. *Musmann and Seiler* [1978] were able to confirm the existence of meridional currents by means of rocket measurements. They observed in some cases peak deflections of the eastward magnetic field component surpassing 400 nT at an altitude of 125 km and a latitude about 3.5° south of the dip equator. This EEJ-related meridional current system is not expected to reach into the F region.

[3] Magsat was the first spacecraft to detect vertically upward flowing currents around altitudes of 400 km above the dip equator in the 17 to 18 local time (LT) sector [e.g., *Maeda et al.*, 1982]. Their typical signature is a bipolar variation in the magnetic field eastward, B_y , component. South of the dip equator one observes a positive and in the north a negative deflection. Peak amplitudes of about ± 10 nT were reached some 8° off the dip equator. *Langel et al.* [1993] interpreted these magnetic features as part of the evening sector EEJ. Alternatively, *Takeda and Maeda* [1983] presented a model, which reproduces the Magsat observations at dusk reasonably well. It considers thermospheric zonal winds as the driver for an F region dynamo. Following the idea of *Rishbeth* [1971] the electric fields generated by the wind at F region heights are mapped down along field lines to the E region. Eastward winds support currents flowing upward over the dip equator, diverting at a certain height along field lines into both hemispheres and closing the meridional loops by equatorward currents at lower altitudes. This scenario is consistent with eastward wind observations during evening hours. For westward winds at F region altitudes, prevailing during earlier times of the day [Wu *et al.*, 1994], loops with an opposite sense of current are expected. So far there has been no observational verification of these day time meridional F region currents.

[4] Among the main open issues with respect to the EEJ is the diurnal variation of the reverse currents and of the E region meridional current loops. Measuring the latter currents is a demanding task. It requires space-borne high-resolution magnetic field vector measurements at an altitude of about 120 km. With respect to the F region dynamo currents, only little is known about its average intensity, diurnal variation and altitude distribution. Due to the poloidal nature of the currents it is necessary to sample the field inside the loop, which means at heights of 500 km and below [Takeda and Maeda, 1983]. The life time of satellite at such a low altitude is generally quite short (e.g., Magsat, 6 months). So far we have only Magsat observations from the evening sector.

[5] We believe that the CHAMP mission can help to answer some of the pending questions. CHAMP was launched on 15 July 2000 into a near-polar (87.3° inclination) near-circular orbit at 456 km altitude. During the first

¹GeoForschungsZentrum Potsdam, Potsdam, Germany.

²Cooperative Institute for Research in Environmental Sciences, University of Colorado, Boulder, Colorado, USA.

4 years the orbit decayed to 380 km. Reentry of the satellite is expected during 2009. Here we consider magnetic field vector data of the first 4 years of the mission to study average features of ionospheric current systems. In an earlier paper Lühr *et al.* [2004] deduced the characteristics of the horizontal electrojet currents around noon from CHAMP scalar magnetic field data. Now looking at vector data from all local times we will (1) validate the earlier EEJ results and (2) investigate the F region meridional current systems.

2. Data Processing Approach

[6] The data used in this study are the magnetic vector components as measured by the Fluxgate magnetometer on CHAMP. This instrument samples all three components of the field at 50 Hz with a resolution of 0.1 nT over a range of $\pm 65,000$ nT. To ensure a high accuracy, the Fluxgate data are routinely calibrated against the absolute scalar Overhauser readings. The measured vector field components are then transformed into the local Cartesian North-East-Down (NEC) system. The angles needed for the transformation from the sensor to the NEC system are provided by a set of star cameras which determine the spacecraft attitude with a resolution of arcseconds.

[7] The quantity of interest for this study is the magnetic field generated by the currents associated with the EEJ and the F region dynamo. For a removal of the geomagnetic field we used the POMME-2.4 model [Maus *et al.*, 2005]. It comprises a spherical harmonic expansion up to degree and order 90 for the static part, to degree 16 for the secular variation and 12 for secular acceleration. A steady magnetospheric field is removed, and the ring current effect, parameterized by D_{ST} , is subtracted. Induction effects caused by these time-varying fields are also considered. Finally, the diamagnetic effect of dense plasmas is corrected according to the approach proposed by Lühr *et al.* [2003]. The electron density and temperature needed for this correction are taken from the Planar Langmuir Probe (PLP) on CHAMP.

[8] The data interval used in this study lasts from August 2000 to October 2004. Only quiet periods with $K_p \leq 2$ have been considered. Since we are interested here in average features of ionospheric currents, data have been averaged over longitude and season at specific local times. The readings are then binned in 1 h local time by 2° corrected geomagnetic (cgm) latitude cells.

[9] Even though most of the background field contributions have been removed there are some systematic variations in the averages, which are predominately caused by large-scale ionospheric currents, such as the Sq system. To remove their influence we have fitted degree 5 polynomials to the latitude profiles of the three component residuals. For this procedure the vicinity of the dip equator ($\pm 14^\circ$ lat) was not considered in the fitting. The obtained polynomials were then subtracted from the data. The magnetic deflections presented thus do not represent the total ionospheric current intensity at the equator but only that part related to local current systems at equatorial latitudes.

[10] In this study we interpret magnetic signatures obtained at a mean altitudes of about 425 ± 40 km to characterize ionospheric currents. Here we focus on the

average diurnal variation. For that reason, the data are not separated by season or longitude. Within the time span of the considered 4 years period, CHAMP visited all located times 11 times. This ensures a good decoupling between seasonal and local time effects. Each bin contains data from about 1000 passes, which is regarded sufficient to provide an average picture of the highly variable current strength.

3. Average EEJ Properties

[11] Latitude profiles of the three magnetic field components are shown in Figure 1, separately for each hour of local time from 6.5 to 19.5 LT. As expected, the B_x component reflects most clearly the EEJ current distribution. The negative deflection is large around noon-time and peaks right at the dip equator. This feature is consistent with the result of earlier EEJ studies from satellites [e.g., Onwumechili and Agu, 1980; Lühr *et al.*, 2004; Le Mouél *et al.*, 2006]. Variations of B_y , as shown in Figure 2, are generally small (note the change in scale). Smaller scale variations during the sun light hours, 7.5–16.5 LT, are an indication of wave features which have not averaged out. Prominent features in this component are bipolar variations occurring around noon and in the evening. These deflections are attributed to an F region meridional current system. Around noon we find a negative-to-positive signature while during the evening hours it has the opposite sense. Extremes are reached at latitudes about 5° off the dip equator. The noon time variations are consistent with downward currents over the dip equator being fed by convergent field-aligned currents (FACs) from both hemispheres. Currents with opposite directions are deduced from the passes during the evening hours, flowing upward at the equator and diverging at a certain height as FACs into both hemispheres. This evening current system resembles that deduced from Magsat data [Takeda and Maeda, 1983]. The latitudinal separation of the extrema in the B_y component increases in the evening sector towards later hours. This means, the upward flowing currents cover a broader latitude range close to the evening terminator.

[12] The B_z component changes sign quite rapidly at the dip equator (Figure 1). The steep plus-minus polarity change from south to north is consistent with the notion of a narrow strip of eastward current. Local extrema appear at $\pm 3.5^\circ$ dip latitude. The latitudes of the B_z extrema coincide quite closely with the boundaries of the eastward electrojet, which are marked by the transition from forward to reverse current density, as found by Lühr *et al.* [2004, Figure 3]. Towards later evening hours the local extrema disappear and the bipolar variations expand to latitudes further away from the dip equator.

[13] In Table 1 the peak-to-peak amplitudes of the three components are listed for every hour. In the case of B_z only the ratio of the ranges, B_{xm}/B_{zm} , is given. The listed amplitude of the B_x deflection reflects the expected diurnal variation of the EEJ intensity. B_y amplitudes are comparably small but significant. The two groups of activity are centered at noon and dusk. Interestingly, the variations around noon are markedly larger than those during the evening hours. The ratio B_{xm}/B_{zm} starts with 1 and then gets progressively smaller towards later hours. An interpre-

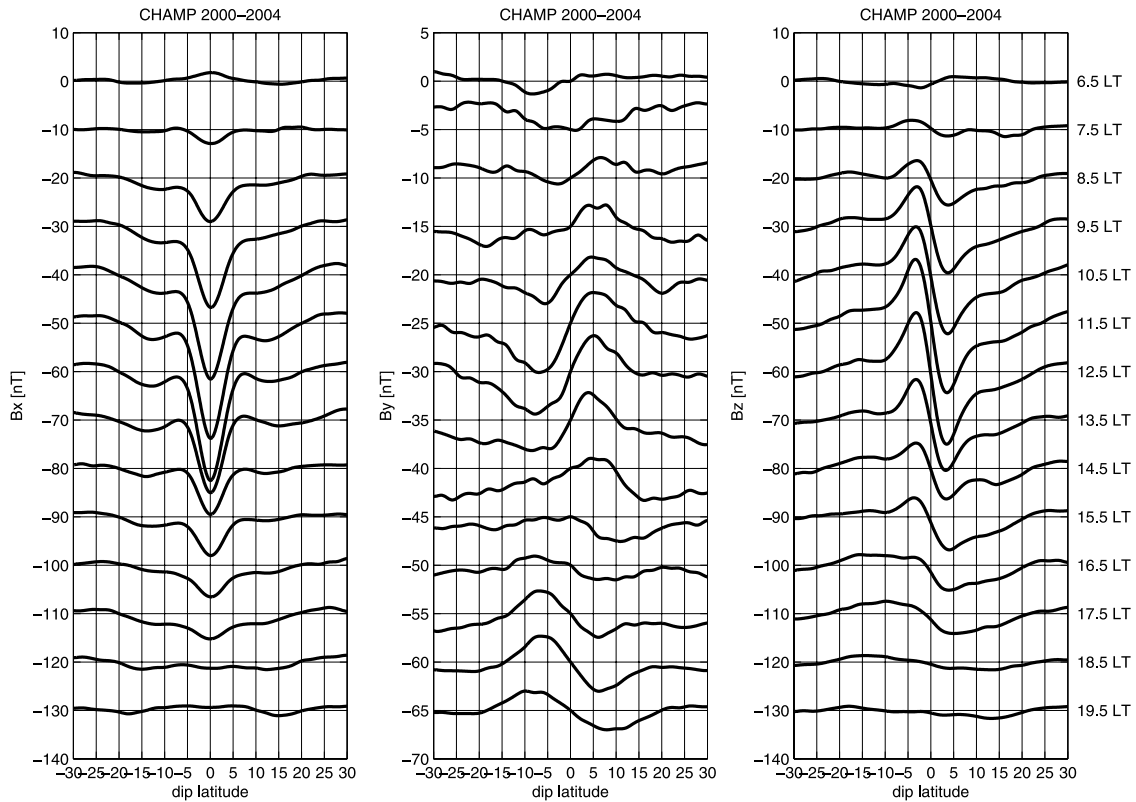


Figure 1. Average magnetic signatures at *F* region altitude caused by equatorial current systems in the B_x (northward), B_y (eastward) and B_z (downward) components. Note the change in scale of the B_y panel. Curves for the different local times (labeled to the right) are offset by 10 nT in case of B_x and B_z , but 5 nT for B_y .

tation of all these observations will be given in the next section.

4. Discussion

[14] In the previous section we presented the average magnetic signatures caused by equatorial ionospheric cur-

rents. To our knowledge, this is the first quantitative vector field study based on satellite data from all dayside local times. *Le Mouél et al.* [2006] also used CHAMP magnetic field vector data but focused on qualitative features of the EEJ, as derived from along-track field gradients. Quantitative features published in previous papers were mostly derived from scalar field satellite measurements [e.g., *Onwumechili and Agu, 1980; Jadhav et al., 2002*]. Spaceborne observations are suited particularly well to identify the spatial structure of the current layer. By direct inversion of the scalar residuals, *Lühr et al.* [2004] derived latitude profiles of the current density. They obtained a strong eastward current at the dip equator and somewhat weaker

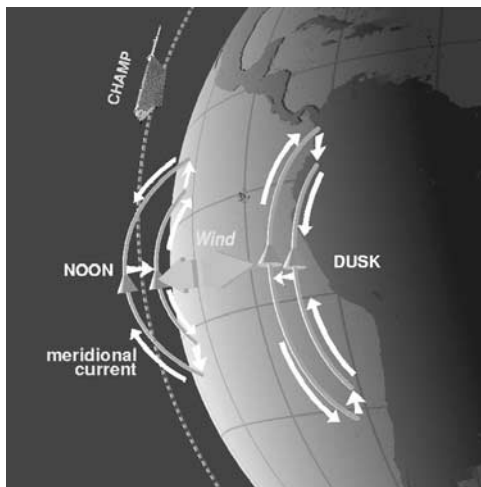


Figure 2. Schematic illustration of the *F* region dynamo over the dip equator driven by thermospheric winds. Meridional current systems are set up both in the noon and dusk sectors.

Table 1. Peak-to-Peak Amplitudes of the Average Magnetic Deflections Caused by the EEJ at 425 km Altitude

Local Time	B_x , nT	B_y , nT	B_x/B_z
6.5	+2.0	–	1
7.5	–3.0	–	1
8.5	–7.5	–	0.77
9.5	–14.0	–	0.80
10.5	–17.9	4.9	0.81
11.5	–22.4	8.3	0.82
12.5	–22.1	8.1	0.82
13.5	–15.3	5.8	0.82
14.5	–9.4	–	0.83
15.5	–7.1	–	0.67
16.5	–5.2	–2.3	0.76
17.5	–3.2	–4.9	0.63
18.5	–	–5.7	–
19.5	–	–3.9	–

reverse currents at both flanks. As a first step, we will test the consistency of their current model with the vector field measurements.

4.1. Features of the EEJ

[15] The first quantity to look at is the ratio of the peak-to-peak amplitudes of B_{xm} and B_{zm} . In case of a single line current, this ratio is 1, as can be deduced from equation (2) of Lühr *et al.* [2004]. The values observed here are generally below 1. Table 1 lists the ratios for the different local time hours. Around noon we find values of about 0.82. This apparent inconsistency may be explained by the effect of the reverse currents. We have taken the average noon-time EEJ current profile presented by Lühr *et al.* [2004, Figure 3] and predicted the ratio B_{xm}/B_{zm} at CHAMP altitude (taking into account the induction effect, as given in their paper). The resulting number is 0.83. This confirms not only the existence of reverse currents but also the quoted ratio of the average current strengths, 65 kA and 21 kA for the forward and reverse currents, respectively. Towards the evening hours the ratios decrease even further. Later we will come back to this point.

[16] Another quantity of interest is the latitude at which B_z peaks. Here again we have used the average EEJ current model of Lühr *et al.* [2004] to predict the locations of the B_z extrema. At CHAMP altitude B_z peaks are expected from the model to coincide with the latitudes of zonal current reversal from eastward to westward at $\pm 3.5^\circ$ dip latitudes. This is exactly where we observe B_z extrema for most of the day. All of these assessments have provided a convincing confirmation for the spatial structure of our noon-time EEJ current model. A comprehensive current model for the evening hours is still missing.

4.2. *F* Region Dynamo

[17] Of particular interest are the signatures of the B_y component. They reflect the intensity of the meridional current system caused by the *F* region dynamo. At first, we compare our results around 18 LT with those of the Magsat dusk passes. The B_y signatures from both missions are in qualitative agreement, exhibiting a positive to negative transition on a northbound pass. The amplitudes are, however, rather different. While we observe a maximum peak-to-peak value in the dusk sector of 6 nT, Magsat data reveal a 3 times larger B_y variation. We estimate that our filter reduces the amplitude in B_y by not more than 1 nT. The amplitude difference may partly be due to the higher solar activity during the Magsat era (F10.7 = 203) compared to the average of the CHAMP period considered here (F10.7 = 153). In addition, Magsat took readings at a somewhat lower orbit. CHAMP data are sampled at a mean height of 425 km. For the Magsat results the quoted altitude is 400 km [Langel *et al.*, 1993]. The dependence of the B_y amplitude on altitude was investigated by Takeda and Maeda [1983] based on Magsat data. From their Figure 6 one can read a reduction of 3 nT (15%) for the 25 km height difference. Also the season may play a role. Magsat missed the summer and fall. All these arguments are probably not sufficient to explain the substantial amplitude difference between the missions, though.

[18] Totally new observations are the B_y signatures around noon. They suggest downward currents in this local

time sector opposed to upward currents at dusk. The range of the eastward component has an amplitude about a factor of 1.5 larger than that in the evening. The observed B_y variations can be used for deriving quantitative characteristics of the meridional current system. For example, the field gradient at the dip equator can be interpreted in terms of vertical current density

$$j_z = \frac{1}{\mu_0} \frac{dB_y}{dx} \quad (1)$$

where dB_y/dx is the meridional gradient of the eastward component. Shortly after noon we observe an along-track field gradient of 1.1 nT/deg. This corresponds to a vertical current density of $j_z = 8 \text{ nA/m}^2$. From the peak-to-peak amplitude of the B_y component the vertical sheet current density, J_z , can be estimated

$$J_z = \Delta B_y / \mu_0 \quad (2)$$

[19] According to Table 1 we find a range, $\Delta B_y = 8 \text{ nT}$ around noon. This gives a downward sheet current density of $J_z = 6 \text{ mA/m}$. The value given here has to be regarded as a lower bound since part of the vertical current may flow below our sampling altitude (380–465 km).

[20] Based on the B_y observations, we suggest a 3-D current system associated with the *F* region dynamo. Following the concept of Rishbeth [1971] we assume vertical polarisation currents over the dip equator driven by thermospheric winds. At the top and the bottom of the affected flux tube currents are diverted along field lines into the *E* regions of both hemispheres. At *E* layer level the meridional currents close. The envisaged geometry of the circuit is shown in Figure 2. Eastward zonal winds cause upward polarisation currents and westward winds downward currents. According to the Horizontal Wind Model (HWM) [Hedin *et al.*, 1991], winds blow westward during most of the day and switch to eastward in the afternoon.

[21] The westward wind around noon is expected to set up, due to dynamo action, an upward pointing electric field over the equator. When mapped down along the field lines the resulting electric field in the *E* layers of both hemispheres points poleward. The strength of the electric field, \mathbf{E} , depends on the ratio between the flux-tube-integrated Pedersen conductivity in the *F* region, \sum_P^F and the sum of the north-south conductances, $2 \sum_P^E$, in the *E* regions of the two hemispheres [Kelley, 1989, section 3.2]

$$\mathbf{E} = \frac{\sum_P^F}{2 \sum_P^E + \sum_P^F} \mathbf{u} \times \mathbf{B} \quad (3)$$

where \mathbf{u} is the zonal wind in the thermosphere and \mathbf{B} is the ambient magnetic field. Highest *F* region conductances are expected on flux tubes containing the equatorial ionisation anomaly (EIA). The average location of the EIA during the afternoon hours was found by Liu *et al.* [2005] in CHAMP data at $\pm 14^\circ$ cgm latitude. The center of the EIA flux tube thus reaches the *E* layer at $\pm 18^\circ$ cgm latitude. The envisaged

current system contains poleward directed Pedersen currents in the *E* region. In case of symmetrical conditions the height integrated Pedersen current density, J_P , in each hemisphere has to be just half of the vertical current density, J_z . Based on this assumption we can estimate the electric field strength and *F* region conductance. For the Pedersen current we can write

$$J_P = \Sigma_P^E E \quad (4)$$

[22] When assuming a noon time *E* region Pedersen conductance of 10 S and inserting the above derived vertical current density, $J_z = 6$ mA/m, we obtain for the electric field, $E = 0.33$ mV/m. Inserting (4) into (3) and considering that the day-time *E* region conductance is much larger than that of the *F* region we may write

$$J_P \approx \frac{1}{2} \Sigma_P^F u B \quad (5)$$

[23] From (5) we see that the current strength is directly proportional to the *F* region conductance but almost independent of the *E* region conditions. This means, the *F* region dynamo acts like a current source. Equation (5) can be solved for the *F* region conductance

$$\Sigma_P^F = J_z / (u B) \quad (6)$$

[24] Inserting typical values for the noon-time zonal wind and B-field, $u = 100$ m/s and $B = 30000$ nT, and taking the above derived vertical current density, we get for the conductance, $\Sigma_P^F = 2$ S. This value is consistent with the conductance of the EIA flux tube as presented by *Heelis* [2004, Figure 11]. Above we mentioned that the range of B_y variation derived from Magsat is three times larger. This implies, when assuming the same zonal wind speed, an *F* region conductance of 6 S, which is exceptionally high and expected only under rather extreme conditions.

[25] For the evening sector we envisage a similar scenario as for the noon time, except that the thermospheric wind is blowing eastward and thus the currents are flowing in the opposite direction. There are, however, strong azimuthal conductivity gradients at the evening terminator, which greatly influence the ionospheric dynamics [*Heelis*, 2004]. For example, the *F* region and with it the EIA flux tube is lifted to higher altitudes. This creates current features covering a wider latitude range at CHAMP altitudes (cf. Figure 2, B_y variations). Also, zonal currents other than the EEJ, flowing at CHAMP heights and above, become important at that time (e.g., gravity-driven currents [*Maus and Lühr*, 2006]). They make the ratio B_{xm}/B_{zm} smaller than would be expected from the EEJ alone (cf. Table 1). During this late time of the day the ratio can thus no longer be used for characterising the EEJ.

[26] The *F* region meridional current system is obviously less affected by the azimuthal conductivity gradient, due to the current source character. We observe a reduction of the B_y range only after 19.5 LT (cf. Figure 2). When the *E* region conductivity is reduced significantly our assumption for equation (5) breaks down. In case the conductance of the *F* region is much higher than that of the *E* region we can make an alternative approximation for equation (3)

$$E \approx u \times B \quad (7)$$

[27] This condition is obviously valid during the night time for hours past 20 LT. Then the *F* region dynamo acts as a voltage source.

[28] A remaining question is, why don't we see clear *F* region dynamo signatures in the B_y component during the morning hours? At that time strong westward winds blow in the thermosphere, but the EIA is not well developed and has not reached CHAMP altitudes. Therefore, no magnetic signature is expected at the present CHAMP altitude. These currents may become visible shortly before re-entry. The lack of B_y variation during the afternoon can be explained by the stagnation of zonal winds in the vicinity of the thermospheric pressure bulge.

[29] In summary, most of the signatures observed in the averaged CHAMP magnetic field components can be explained by equatorial current features such as the EEJ and the *F* region meridional currents. In particular for the *F* region dynamo, we have provided the first observational evidence for the currents at all local times.

[30] **Acknowledgments.** We thank P. Ritter and M. Rother for their help in preparing the figures. The operational support of the CHAMP mission by the German Aerospace Center (DLR) and the financial support for the data processing by the Federal Ministry of Education and Research (BMBF) are gratefully acknowledged.

References

- Fambitakoye, O., and P. N. Mayaud (1976), Equatorial electrojet and regular daily variation S_R : I. A determination of the equatorial electrojet parameters, *J. Atmos. Terr. Phys.*, *38*, 1–17.
- Hedin, A. E., et al. (1991), Revised global model of thermospheric winds using satellite and ground-based observations, *J. Geophys. Res.*, *96*, 7657–7688.
- Heelis, R. A. (2004), Electrodynamics in the low and middle latitude ionosphere: A tutorial, *J. Atmos. Sol. Terr. Phys.*, *66*, 825–838.
- Jadhav, G., M. Rajaram, and R. Rajaram (2002), A detailed study of equatorial electrojet phenomena using Ørsted satellite observations, *J. Geophys. Res.*, *107*(A8), 1175, doi:10.1029/2001JA000183.
- Kelley, M. C. (1989), *The Earth's Ionosphere*, Elsevier, New York.
- Langel, R. A., M. Purucker, and M. Rajaram (1993), The equatorial electrojet and associated currents as seen in Magsat data, *J. Atmos. Terr. Phys.*, *55*, 1233–1269.
- Le Mouél, J.-P., P. Shebalin, and A. Chulliat (2006), The field of the equatorial electrojet from CHAMP data, *Ann. Geophys.*, *24*, 515–527.
- Liu, H., H. Lühr, V. Henize, and W. Köhler (2005), Global distribution of the thermospheric total mass density derived from CHAMP, *J. Geophys. Res.*, *110*, A04301, doi:10.1029/2004JA010741.
- Lühr, H., M. Rother, S. Maus, W. Mai, and D. Cooke (2003), The diamagnetic effect of the equatorial Appleton anomaly: Its characteristics and impact on geomagnetic field modelling, *Geophys. Res. Lett.*, *30*(17), 1906, doi:10.1029/2003GL017407.
- Lühr, H., S. Maus, and M. Rother (2004), Noon-time equatorial electrojet: Its spatial features as determined by the CHAMP satellite, *J. Geophys. Res.*, *109*, A01306, doi:10.1029/2002JA009656.
- Maeda, H., T. Iyemori, T. Araki, and T. Kamei (1982), New evidence of a meridional current system in the equatorial ionosphere, *Geophys. Res. Lett.*, *9*, 337–340.
- Maus, S., and H. Lühr (2006), A gravity-driven electric current in the Earth's ionosphere identified in CHAMP satellite magnetic measurements, *Geophys. Res. Lett.*, *33*, L02812, doi:10.1029/2005GL024436.
- Maus, S., H. Lühr, G. Balasis, M. Rother, and M. Manda (2005), Introducing POMME, The Potsdam Magnetic Model of the Earth, in *Earth Observation With CHAMP*, edited by C. Reigber et al., pp. 293–298, Springer, New York.
- Musmann, G., and E. Seiler (1978), Detection of meridional currents in the equatorial ionosphere, *J. Geophys.*, *44*, 357–372.
- Onwumechili, C., and C. Agu (1980), General features of the magnetic field of the equatorial electrojet measured by the POGO satellites, *Planet. Space Sci.*, *28*, 1125–1130.
- Rishbeth, H. (1971), The *F*-layer dynamo, *Planet. Space Sci.*, *19*, 263–267.

- Sugiura, M., and D. J. Poros (1969), An improved model equatorial electrojet with a meridional current system, *J. Geophys. Res.*, *74*, 4025–4034.
- Takeda, M., and H. Maeda (1983), *F*-region dynamo in the evening— Interpretation of equatorial ΔD anomaly found by Magsat, *J. Atmos. Terr. Phys.*, *45*, 401–408.
- Untiedt, J. (1967), A model of the equatorial electrojet involving meridional currents, *J. Geophys. Res.*, *72*, 5799–5810.
- Wu, Q., T. L. Killeen, and N. W. Spencer (1994), Dynamics Explorer 2 observation of equatorial thermospheric winds and temperatures: Local time and longitude dependence, *J. Geophys. Res.*, *99*, 6277–6288.
-
- H. Lühr, GeoForschungsZentrum Potsdam, Telegrafenberg, Haus G, D-14473 Potsdam, Germany. (hluehr@gfz-potsdam.de)
- S. Maus, Cooperative Institute for Research in Environmental Sciences, University of Colorado, 216 UCB, Boulder, CO 80309, USA.